

A Soma Segmentation Benchmark in Full Adult Fly Brain

Xiaoyu Liu¹ Bo Hu¹ Mingxing Li¹ Wei Huang¹ Yueyi Zhang^{1,2} Zhiwei Xiong^{1,2,*}

¹University of Science and Technology of China

²Institute of Artificial Intelligence, Hefei Comprehensive National Science Center

{liuxyu, hubosist, mxli, weih527}@email.ustc.edu.cn, {zhyuey, zwxiong}@ustc.edu.cn

Abstract

Neuron reconstruction in a full adult fly brain from high-resolution electron microscopy (EM) data is regarded as a cornerstone for neuroscientists to explore how neurons inspire intelligence. As the central part of neurons, somas in the full brain indicate the origin of neurogenesis and neural functions. However, due to the absence of EM datasets specifically annotated for somas, existing deep learning-based neuron reconstruction methods cannot directly provide accurate soma distribution and morphology. Moreover, full brain neuron reconstruction remains extremely time-consuming due to the unprecedentedly large size of EM data. In this paper, we develop an efficient soma reconstruction method for obtaining accurate soma distribution and morphology information in a full adult fly brain. To this end, we first make a high-resolution EM dataset with fine-grained 3D manual annotations on somas. Relying on this dataset, we propose an efficient, two-stage deep learning algorithm for predicting accurate locations and boundaries of 3D soma instances. Further, we deploy a parallelized, high-throughput data processing pipeline for executing the above algorithm on the full brain. Finally, we provide quantitative and qualitative benchmark comparisons on the testset to validate the superiority of the proposed method, as well as preliminary statistics of the reconstructed somas in the full adult fly brain from the biological perspective. We release our code and dataset at <https://github.com/liuxy1103/EMADS>.

1. Introduction

Drosophila melanogaster, also known as the fruit fly, is an organism with intelligent behaviors including perception, learning, and judgment [10, 34, 36]. It has a complete and relatively simple neural system [6, 37]. The interactions among neurons in the system guide the *drosophila*'s intelligent behaviors [8, 14, 23, 35]. Therefore, the study

of *drosophila* neurons, which has fascinated neuroscientists for more than a century [5, 7, 16, 40, 44], has key implications for understanding how the brains of living organisms produce intelligence [2, 41].

As the central part of the neuron, the soma maintains the neuron structure and controls the formation of neurites [22, 30]. Studies have shown that the location and morphology of somas in the full brain are related to neural development and the neural logic function [3, 17], and the number of somas is related to the complexity of the brain and the age of the living body [1, 25]. Therefore, it is of great biological significance to investigate soma reconstruction in the full brain of model organisms such as *drosophila*.

Traditional studies in this field are mainly based on brain images collected by optical microscopies [13, 38]. The soma structure is first stained with specific staining proteins, and the confocal images collected could show fluorescence staining signals, so as to obtain the soma distribution of the full brain of *drosophila*. However, the resolution of confocal images is low, making it difficult to obtain the exact morphology of each soma. Based on the assumption that each cell has only one nucleus, the isotropic fractionator method [15, 18] is used to obtain the number of somas in the full brain of *drosophila*. This method destroys the brain structure during the production of cell suspension, so the distribution of somas in the full brain cannot be obtained.

Recently, with the development of high-speed electron microscopy (EM) scanning technology, high-resolution EM image datasets of different species including *drosophila* [42], mouse [31], and human [39] have been successfully acquired, and the full adult fly brain (FAFB) dataset [47] imaged from a complete *drosophila* brain can be regarded as a representative. Based on these datasets, advanced deep learning algorithms are developed to automatically reconstruct neurons [12, 23] and cell nucleus [32] in EM images for connectomics study. Meanwhile, parallel and distributed data processing pipelines [39, 46] are proposed to deploy these algorithms on large-scale EM datasets. However, due to the lack of high-resolution EM datasets specifically annotated for somas, existing works

*Corresponding author.

cannot directly provide accurate soma distribution and morphology information.

In this paper, we make one of the first efforts to develop an efficient soma reconstruction method in a full adult fly brain, aiming to obtain accurate soma distribution and morphology information for this model organism. The contributions of this work are four aspects:

- We make a high-resolution EM soma dataset with fine-grained 3D manual annotations for more than 8×10^9 voxels. To the best of our knowledge, this dataset is the first of its kind.
- Relying on the above dataset, we propose an efficient, two-stage deep learning algorithm for soma instance segmentation, and benchmark existing alternative methods to validate the superiority of ours.
- We deploy a parallelized, high-throughput data processing pipeline for executing our algorithm on the full brain, fulfilling the soma reconstruction task on a 90-GPU cluster within 4 days.
- We provide quantitative and qualitative results for evaluating the accuracy and efficiency of the proposed method, along with preliminary statistics of the reconstructed somas in the full adult fly brain, including count, size, distribution and morphology.

We believe our work will contribute to the study of the drosophila neural system. The benchmark dataset has been released to facilitate future research along this line. Code and a 4K video of the full brain reconstruction result are now available through the links provided in Github website.

2. Related Work

2.1. Neuron Reconstruction

Recent works of neuron reconstruction in EM images, such as FFN [23], MALA [12], and other elaborate methods [19, 20, 24, 28, 29], embrace the power of deep learning and obtain neuron instance information based on connectivity, pre-labeling, etc. However, due to the absence of elaborate annotations and specific designs for somas in these algorithms, the shape and position of the soma cannot be accurately predicted. Moreover, these algorithms are generally time-consuming when dealing with extremely large-scale EM data. For example, MALA has complex post-processing procedures based on optimization of traditional methods, and FFN has a very large number of sliding windows during inference, making them inefficient for fast soma reconstruction in the full brain of drosophila. More recent works [11, 26] reconstruct all neurons on the FAFB dataset. However, one cannot directly obtain the accurate distribution and morphology information of somas based on these results, since each generated segment often contains all parts of a fly neuron: a soma, dendrites, axon ter-

minals, and a primary neurite. Therefore, our work on independent soma reconstruction is complementary to neuron reconstruction for connectomics study.

2.2. 3D Nuclei Reconstruction

As a parallel line, there are two recent works on nucleus reconstruction in EM images. Although the soma has a one-to-one correspondence to the nucleus, the nucleus is often located in the center of the soma with a regular spherical shape, which cannot reflect the morphology of the soma. Mu et al. [32] reconstruct all cell nuclei on the FAFB dataset by using a standard 2D U-Net to predict the binary classification of individual pixels as either nucleus or not. However, this method lacks the utilization of 3D structural information and is difficult to apply to densely distributed somas with complex shapes. Lin et al. [27] make a neuronal nuclei instance segmentation EM dataset at the sub-cubic millimeter scale and propose a hybrid representation segmentation method by directly adopting a 3D model to predict multiple complete objects simultaneously. However, this method is not suitable for high-resolution EM images at the nanometer scale, since somas with much larger sizes cannot be processed by the model due to the limited GPU memory. Different from existing nucleus segmentation methods, our proposed soma segmentation method not only adopts a 3D model to consider the 3D structure of complete somas but also can directly process high-resolution EM images with an elaborate two-stage instance segmentation algorithm.

3. EM Dataset with Fine-Grained Annotations

We make an EM adult drosophila soma (EMADS) dataset with fine-grained manual annotations. EMADS contains 204 completely annotated 3D somas with different sizes and morphologies derived from 10 apart regions in a full adult fly brain.

3.1. Source and Preparation

The EM images of the adult drosophila brain that we annotate originate from FAFB [47]. FAFB is the world's first EM dataset for a complete drosophila brain. FAFB is imaged at the synaptic resolution and has been processed with stitching and alignment. There are a total of 7,062 sections in FAFB, and the full resolution of each section is $286,720 \times 155,648$ which is partitioned into $8,192 \times 8,192$ images, resulting in 40 TB data in storage. Thanks to the high-resolution imaging technique, biological structures and boundaries in FAFB are clear, making fine-grained manual annotations on the voxel-level data possible. However, the annotation workload on such high-resolution, large-scale data is heavy. Before annotation, we first downsample FAFB at both the x -axis and the y -axis with a factor of 4. The physical resolution of the downsampled dataset is $16\text{nm} \times 16\text{nm} \times 40\text{nm}$ ($x \times y \times z$). In this

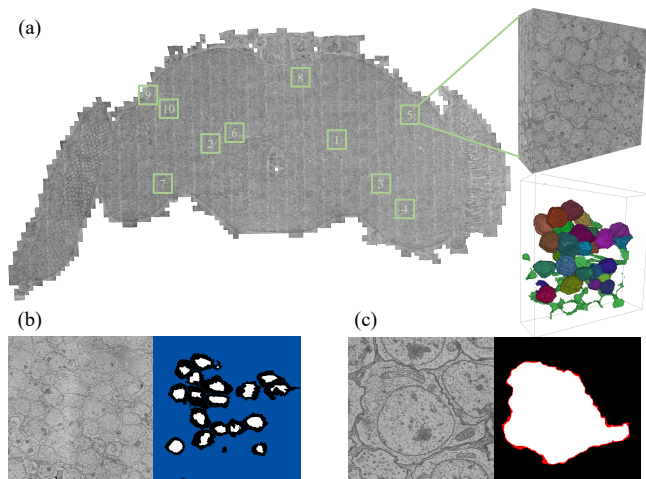


Figure 1. (a) An overview of the FAFB dataset. We select 10 EM blocks from the full brain, and annotate them to make our label sets. We use different colors to represent different soma instances, and the green color indicates the annotated background region. (b) A visualization example for our localization label set. The white and black colors indicate the seed and non-seed annotations, respectively. The area in blue color is unannotated. (c) A visualization example of the segmentation label set. The white and black colors indicate the soma-of-interest and background annotations, respectively. The red color indicates the boundary annotation of the soma-of-interest. For simplicity and clarity, we visualize (b) as a slice of the 3D block and (c) as a slice of the 3D patch.

way, the annotation workload for each soma is lessened so that we can annotate more somas in diverse sizes and morphologies. Besides, the reduced resolution also lessens the computational burden in our method and makes it affordable for 3D deep networks. We store the full brain data in our defined 3D image blocks, and the size of each block is $1,836 \times 1,836 \times 186$. The 3D image blocks are arranged in the order of x, y (in the lateral direction) and z (in the axial direction) axis. By loading these blocks in the axial orders continuously, we can obtain the full brain data. The parallel data processing pipeline in our method is detailed in Sec. 5.

3.2. Selective Annotations

Many previous works [9, 21] utilize specific biological stains to mark somas from 3D confocal images to indicate a general soma distribution in the full drosophila brain. Depending on this distribution, we select 10 apart image blocks from FAFB according to the location and density of somas in the full brain. We then organize a group of human annotators to annotate a part of somas and background areas inside these 10 image blocks, with an efficient and semi-automatic annotation tool VAST [4]. The annotations are conducted at the voxel level, with the boundary of somas to be annotated precisely. 20 master and Ph.D. students majoring in neuroscience or computer vision devote them-

selves to this annotation task. We annotate 204 complete somas with different sizes and morphologies inside these 10 image blocks, and each soma takes more than two hours for one person to annotate. All 10 blocks are used to ensure the diversity of soma distribution and morphology. At the same time, weighing the workload of the annotators and the amount of data to be annotated, we only annotate about 20 somas in each block, and there are still unlabeled areas. The total number of annotated voxels is more than 8×10^9 . The average size of these somas is around $300 \times 300 \times 100 \text{ voxel}^3$. The annotations are instance-wise, which means each soma has a unique instance number that is different from other somas. After the group annotation, two experts check every annotated soma in a cross manner, and correct the annotation mistakes. Finally, we obtain 10 EM blocks with 10 corresponding label blocks, each with a resolution of $1,836 \times 1,836 \times 186$. We visualize one of these blocks as an example in Fig. 1(a). Given that the soma is continuous with the neurites that emanate from it, we annotate each soma until its cell membrane curve narrows significantly and reaches plateaus.

3.3. Localization Label Set

We first employ our annotations to make a label set for localizing somas in a given EM block. We perform a binary morphological erosion operation on the annotation of each soma in its corresponding label block. Through this operation, the eroded annotations of somas are labeled as instance seeds, which provides location information for each annotated soma. In addition, since the erosion operation preserves the morphology of each soma to a certain extent, we can obtain the rough size of the soma according to the size of the corresponding instance seed. After that, each labeled block in the localization label set consists of two types of labels besides the unannotated areas. These two labels denote the instance seeds of the annotated somas and the non-seed areas (which can be either the erosion areas or the non-soma areas). An example is given in Fig. 1(b). This localization label set, stored in blocks with a uniform size after further downsampling, is used to localize somas in an efficient way in the first stage of our segmentation algorithm (see details in Sec. 4).

3.4. Segmentation Label Set

We then employ our partially annotated blocks to make the other label set for segmenting somas from patches. Specifically, we crop the annotated somas from their blocks to patches. The size of each patch is slightly larger than the size of the soma, and each soma is at the center of its patch. Since many somas are next to each other and thus it is hard to distinguish instances, we devise the segmentation label set with three types of labels to tackle this problem. We erode the annotation of each soma inside its patch by

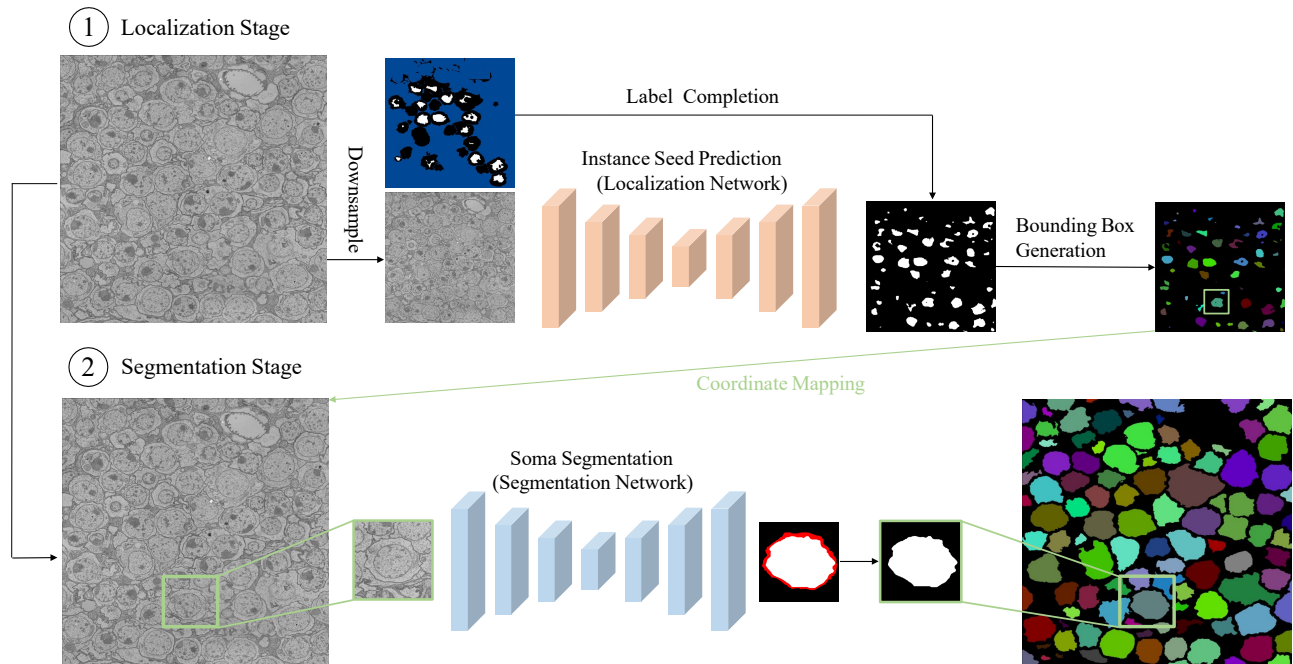


Figure 2. Illustration of our proposed soma instance segmentation algorithm. The localization stage aims to localize somas by predicting instance seeds and generating bounding boxes for them in a given EM block, and the segmentation stage aims to segment somas from the predicted bounding boxes.

two voxels. We then label the eroded soma at the center of the patch as the soma-of-interest, and label the erosion area as the soma boundary. The rest area in a patch except for the soma-of-interest and the soma boundary is regarded as a separate label. Therefore, the segmentation label set consists of three types of segmentation labels. An example is given in Fig. 1(c). This segmentation label set, stored in patches with variable sizes, is used to segment somas in an accurate way in the second stage of our segmentation algorithm (see details in Sec. 4).

4. Two-Stage Soma Segmentation Algorithm

We propose an accurate and efficient soma instance segmentation algorithm. Our algorithm contains two sequential stages, the localization stage and the segmentation stage. The localization stage aims to localize somas by predicting instance seeds and generating bounding boxes for them in a given EM block, and the segmentation stage aims to segment the complete soma (soma-of-interest) located in the center of the predicted bounding boxes. These bounding boxes provide 3D soma candidates for the segmentation stage, which filter out regions without soma and speed up soma reconstruction in the whole brain. We illustrate the proposed algorithm in Fig. 2.

4.1. Localization Stage

The localization stage consists of three steps: label completion, bounding box prediction and coordinate mapping.

First, we complete the labels for the unannotated areas in our localization label set automatically with a localization network using the U-Net model. Then, we adopt the completed label set to continually train this U-Net model to predict instance seeds of the somas in unseen blocks, and generate the bounding boxes for the somas by the instance seeds. Finally, we map the bounding boxes back to the original blocks. The following segmentation stage segments somas from these bounding boxes. We illustrate the detailed structures of our networks and training details in supplementary materials.

Label Completion and Instance Seed Prediction. The localization label set is stored after downsampling so that we can feed a full EM block into our localization network within the capacity of GPU memories. The factors of downsampling are 4, 4 and 6 for x -, y - and z -axis, respectively, resulting in a uniform block size of $459 \times 459 \times 62$. Despite that we have labels for a part of the areas in our localization label set, there are still unannotated areas without labels. We thus use our localization label set to train a network to classify the instance seeds of somas and the non-seed areas on the labeled areas. First, we ignore the unannotated areas and use the original labels to optimize the network. The optimization only computes loss on the labeled areas. After the optimization converges, we employ the network to predict results for the unannotated areas. We combine both the generated labels and the original labels together to form the final labels for each block. We then adopt the final la-

bels to further optimize the network until convergence. The training details are shown in supplementary materials.

Bounding Box Generation. After label completion, we obtain a trained classification network. We then use it to predict instance seeds of somas for unseen EM blocks. According to the sizes of the predicted instance seeds, our method automatically generates the 3D bounding boxes for somas that the instance seeds indicate. We set the centroid of the predicted instance seed as the center for the bounding box. The length of each border of the 3D bounding box is predefined as more than two times the instance seed, which can generally cover the corresponding soma completely. Each bounding box thus indicates a patch that contains a complete soma.

Coordinate Mapping. After obtaining the bounding boxes for somas in a given block, we can localize the somas. However, since the block we use to localize somas has been downsampled before, we have to map the coordinate back to the original block. We multiply the coordinate by the downsampling factors 4, 4 and 6, and adopt the bounding boxes with the multiplied coordinates to localize the somas in the original block.

4.2. Segmentation Stage

In the segmentation stage, we train a segmentation network using the U-Net backbone (which can be readily upgraded to more advanced structures such as transformer, as shown in Sec. 6) on our segmentation label set to classify the soma-of-interest, the soma boundary and the rest area from a given patch. Note that the network only predicts the complete soma at the center of the patch, and the rest area is regarded as the background. Based on this special design, we can directly train a 3D model on the partially annotated dataset. Moreover, this design is beneficial for dealing with densely distributed somas, since it is difficult to directly predict the background between adjacent somas, even on fully annotated datasets. During inference, we regard the bounding boxes we obtain in the localization stage as the patches, and employ the trained segmentation network to predict voxel-wise classes for these patches. Since the size of each patch is variable, we set the batch size as 1 during network training. Finally, we take the predicted soma-of-interest class as our soma segmentation results.

5. Parallelized Large-scale Data Processing

To cope with the huge amount of EM data of a full adult fly brain and accelerate the computation, we deploy a parallelized, high-throughput data processing pipeline on distributed clusters of CPUs and GPUs, which is shown in supplementary materials. Overall, our pipeline follows the design of a mainstream distributed processing algorithm [46] but is customized based on our local infrastructure and our soma segmentation task. Firstly, we divide the whole FAFB

volume into a number of 3D blocks. Secondly, we execute a segmentation procedure to extract somas within each block in parallel. Thirdly, we stitch all block-wise segmentation results to obtain the final reconstruction result for the whole 3D volume.

3D Block Division. Limited by the RAM size, it is impossible to process the whole FAFB volume directly in a single cluster node. We divide the whole 3D volume into overlapping 3D blocks and save them in our purpose-built data center. Then the cluster nodes process these blocks in parallel. Metadata, containing the relative location in the whole 3D volume, accompanies each block. In total, we generate 40,590 blocks with a size of $1,836 \times 1,836 \times 186$ voxel from the whole FAFB volume. Neighboring blocks share an overlapping region with 212×30 voxels in lateral and axial directions, respectively, which are used for stitching the blocks later.

Intra-block Segmentation. We package these divided blocks into groups, each of which can be distributed to and processed by a computing task with one TITAN XP GPU and corresponding CPUs, RAM, *etc.* We develop a task management front-end to produce and submit these tasks to a task queuing system. All tasks are executed independently to process groups of blocks by the above deep learning-based soma segmentation algorithm. This processing stage requires little inter-process communication. Finally, each task generates a group of intra-block segmentation results and writes them into our data center for the following processing stage.

Inter-block Stitching. To obtain the complete segmentation result of one soma instance across different neighboring blocks, we adopt a hierarchical block stitching algorithm with three steps to stitch the segmentation results efficiently. Firstly, we compute the overlap ratio of each soma between two adjacent blocks. If the overlap ratio exceeds an empirically predetermined threshold, we consider it to be a soma spanning two blocks. In other words, these two somas with different IDs should be merged, *i.e.*, they should be with the same ID. Note that, in order to realize the stitching process in parallel, we store the IDs that need to be merged into a shared list instead of immediately changing the IDs in the current block. Secondly, we unify the pairing of all IDs in the shared list to ensure that each ID that needs to be merged corresponds to a unique target ID. Finally, we remap the IDs of somas in all blocks according to the shared list. The inter-block stitching step is implemented in a parallel manner, and the details are shown in supplementary materials.

6. Experimental Results

6.1. Visualization Results

We first provide some visualization results for the full brain soma reconstruction, as shown in Fig. 3. Following

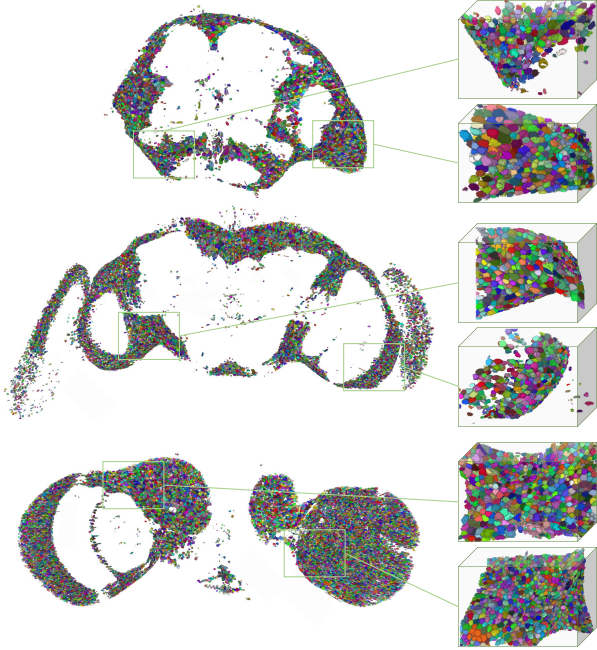


Figure 3. Visualization of our soma reconstruction for a full adult drosophila brain. Each color instance corresponds to a reconstructed soma.

the z -axis order in the FAFB dataset, we select three 3D sections of the full brain soma reconstruction results as an example, and show the details in two representative regions, respectively. Moreover, we give a 4K video in supplementary materials for the complete reconstruction results.

6.2. Quantitative Results

To validate the effectiveness and efficiency of the proposed method, we compare our method with two existing methods for nucleus reconstruction in EM images, *i.e.*, Mu et al. [32] and Lin et al. [27]. To adapt these two methods to our EMADS dataset, we only use the annotated areas to optimize the networks and ignore the unannotated areas. For the second method, we have to downsample the dataset to 1/96 of the previous volume so that each block can be fed to a standard 3D U-Net as the method requires. Then, the segmentation result is upsampled to the previous scale. In addition, we compare our method with two self-designed baseline methods. Baseline 1 adopts dense sliding bounding boxes in a uniform size on the EM block instead of localization, and utilizes a two-class network to segment the somas and the rest areas. Baseline 2 is similar to Baseline 1, and the only difference is that it adopts a three-class network for segmentation. After the dense sliding finishes, the segmented somas are endowed with instances by their connected components in the block.

Evaluation Datasets and Metrics. We fully annotate the somas in two additional EM blocks named A and B, each of which contains about 50 somas. They are non-overlapping

with the 10 training blocks in EMADS, serving as the evaluation blocks. The somas in different blocks have different sizes and morphologies. The background areas are also of different types. We adopt 3D Average Precision metrics [45], *i.e.*, mAP and mAP₅₀ as the instance segmentation metrics to evaluate the instance localization and segmentation performance. In addition, we also use the Jaccard score [33] as the semantic segmentation metric to evaluate the semantic segmentation performance.

Comparison with Existing Methods. As shown in Table 1, compared with the two existing methods for nucleus reconstruction, our method with the U-Net backbone achieves much better performance in terms of the instance segmentation metrics mAP and mAP₅₀, due to its special design tailored for the soma reconstruction task. It should be noticed that, however, these two existing methods perform not badly in terms of the semantic segmentation metric, which suggests that they mainly fail to distinguish between soma instances. This can be verified by visual comparison examples in Fig. 4. As can be seen, our results with fewer segmentation errors provide more accurate distribution and morphology information of somas.

Comparison with Baseline Methods. Compared with Baseline 1 and Baseline 2, our method is about 6 times faster and achieves better performance, which validates the efficiency of the localization stage in our method. We also provide visual comparison examples with the two baseline methods in supplementary materials. To further demonstrate the generality of our method, we upgrade the 3D U-Net used in the segmentation stage to the state-of-the-art backbone based on the transformer architecture, *i.e.*, Swin-UNETER [43]. The result of ‘Ours-Swin’ proves that thanks to the flexibility of our two-stage segmentation algorithm, a more powerful backbone network brings new performance improvements.

6.3. Ablation on Seed Size

When we make our localization label set, we need to erode the annotated somas to obtain the instance seeds. The sizes of the instance seeds are different when we adopt different erosion operations. We thus conduct an ablation study on seed size. The seed size denotes the maximum number of voxels a seed contains. The ablation results are shown in Table 2, which demonstrates that the seed size of 50 provides the best performance.

7. Statistics

We compile statistics for the reconstructed somas in the full adult fly brain in four aspects: count, size, distribution and morphology. To make the reconstructed somas correspond to the neurobiological structures in the brain, we partition the full brain into four types of cubic regions: the optic lobes, and the central brain A, B and C as shown in the

Method	Test block A			Test block B			Average			time
	mAP	mAP ₅₀	Jacc.	mAP	mAP ₅₀	Jacc.	mAP	mAP ₅₀	Jacc.	
Mu et al.	0.045	0.212	0.579	0.072	0.219	0.578	0.059	0.216	0.579	63s
Lin et al.	0.017	0.096	0.420	0.020	0.093	0.397	0.019	0.095	0.409	32s
Baseline 1	0.213	0.699	0.587	0.179	0.680	0.524	0.196	0.690	0.556	960s
Baseline 2	0.226	0.695	0.592	0.242	0.709	0.558	0.234	0.702	0.575	1142s
Ours-UNet	0.301	0.713	0.638	0.302	0.721	0.590	0.301	0.717	0.614	178s
Ours-Swin	0.420	0.853	0.650	0.303	0.614	0.474	0.362	0.734	0.562	158s

Table 1. Quantitative comparison results with existing and baseline methods.

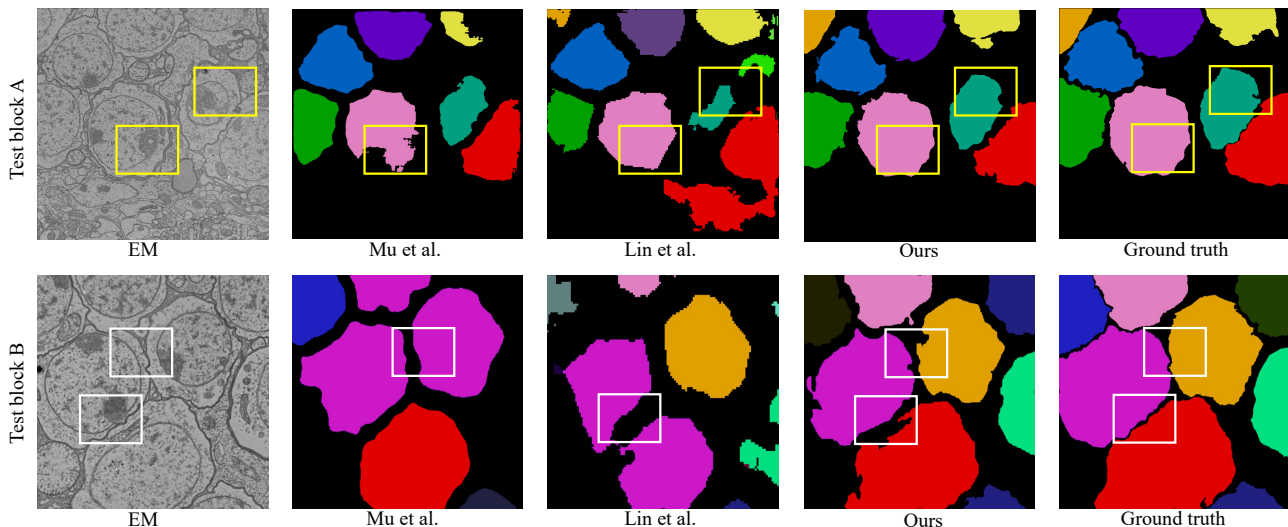


Figure 4. Visual comparison results of our method and two existing methods. The yellow box and the white box indicate the segmentation and localization errors.

top left in Fig. 5. We compute the statistical results for each of them. More details of the brain partitions are shown in supplementary materials. According to the official nomenclature of brain structures for the drosophila [21], the central brain A contains superior neuropils (SNP), mushroom bodies (MB), inferior neuropils (INP), central complex (CX) and lateral horn (LH); the central brain B contains ventrolateral neuropils (VLNP), ventromedial neuropils (VMNP), antennal lobes (AL), and lateral complex (LX); the central brain C contains periesophageal neuropils (PENP), gnathic ganglia (GNG) and external nerves.

Soma Count. The number of soma instances we reconstruct from the full adult fly brain is 116,761. This number is basically consistent with the result in the recent nucleus reconstruction work [32] and the result reported by a traditional method [15]. Regarding the count in each region, the optic lobes contain the majority of somas in the full brain with a number of 76,316. The central brains A, B and C contain 18,313, 14,424 and 7,708 somas, respectively. The number of somas in the central brain A is obviously more than that of B and C due to the abundant Kenyon cells in the mushroom body [21].

Soma Size. We illustrate the counts of somas in different sizes of each region in the second row of Fig. 5. The largest

soma in the full brain has a size of $980 \mu m^3$, and most of the soma sizes are less than $75 \mu m^3$. The mean soma size in the full brain is $27 \mu m^3$. The mean sizes of somas in the central brain A, B, C and the optic lobes are 39, 35, 29 and $23 \mu m^3$, respectively.

Soma Distribution. From Fig. 3, we can observe that the somas mainly locate at the rind of the full brain, and a few somas locate at the center of the brain. The results in Fig. 5 demonstrate that the optic lobes have the most somas, while the central brain C has the fewest somas. The statistical results are consistent with the visualization results.

Soma Morphology. Somas in different morphologies have different diameters (*i.e.*, the maximum length of its spatial size). We count the somas in different diameters. The soma diameters are basically consistent in the four regions, as shown in the third row in Fig. 5. The somas in the optic lobes have the smallest mean diameter, which corresponds to the fact that there are much more neural stem cells that are undifferentiated in this region than in the central brain A, B and C, as introduced in [22]. Moreover, we count somas in different diameter ratios (*i.e.*, ratios between the maximum and the minimum lengths of its spatial size), which reflects the roundness of the sphere. As shown in the fourth row in Fig. 5, the somas in the optic lobes have the maximum

Size	Test block A			Test block B			Average		
	mAP	mAP ₅₀	Jacc.	mAP	mAP ₅₀	Jacc.	mAP	mAP ₅₀	Jacc.
80	0.261	0.696	0.606	0.276	0.728	0.574	0.269	0.712	0.590
50 (Ours)	0.301	0.713	0.638	0.302	0.721	0.590	0.302	0.717	0.614
10	0.284	0.715	0.625	0.246	0.667	0.579	0.265	0.691	0.602

Table 2. Ablation study on seed size.

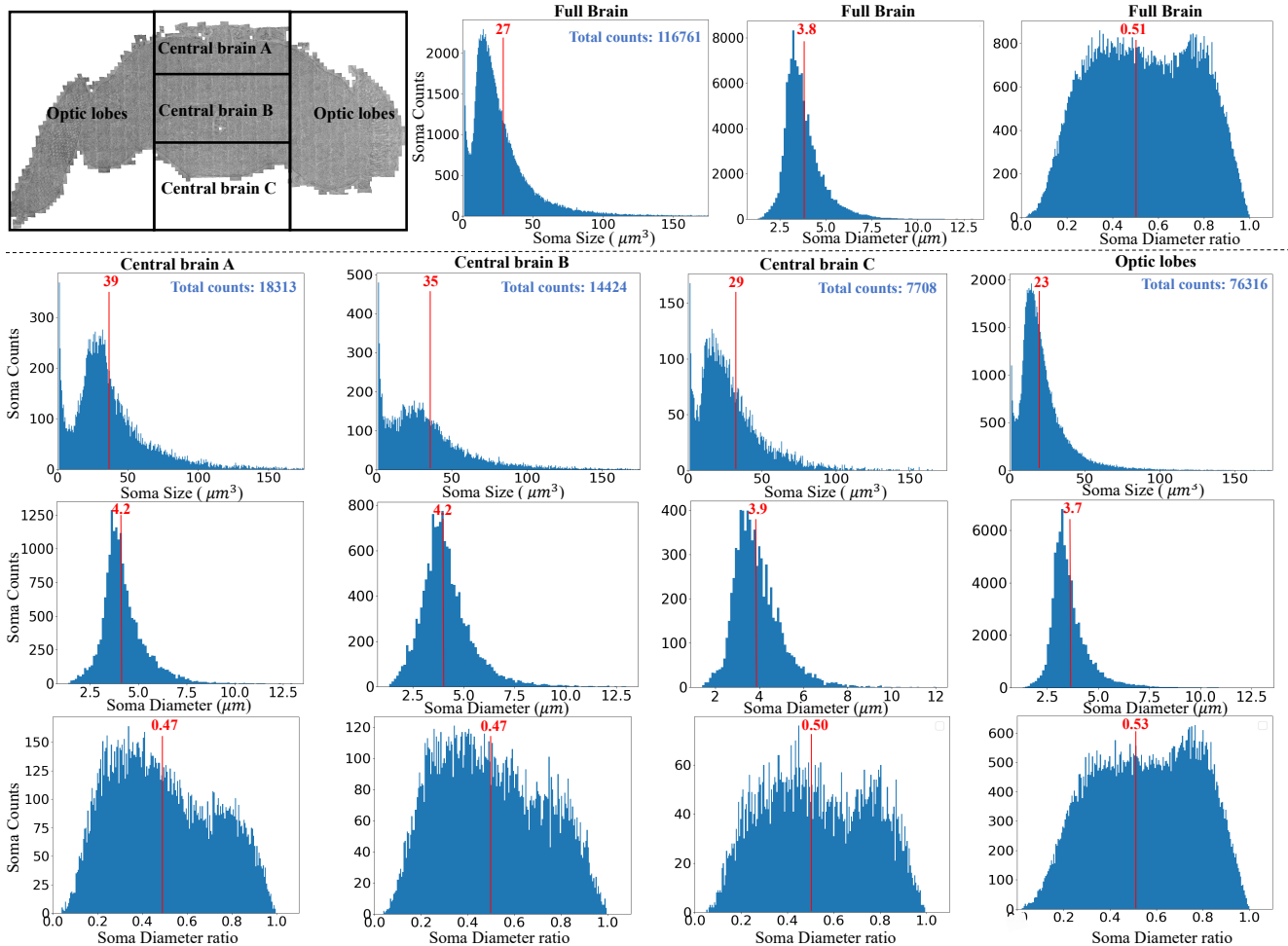


Figure 5. Statistics of soma sizes and diameters in different regions of the full brain. The first row illustrates our separated four types of regions and the statistical results on the full brain. The second row illustrates the soma count in different sizes, the third row illustrates the soma count in different soma diameters, and the fourth row illustrates the soma count in different diameter ratios. The red line highlights the mean value of each statistic.

mean diameter ratio and the morphology of these somas is more similar to the sphere.

8. Conclusion

In this paper, we made one of the first efforts to develop an accurate and efficient soma reconstruction method for a full adult fly brain. We first contribute the EMADS dataset with fine-grained annotation on somas, based on which we then propose an efficient, two-stage deep learning algorithm for accurate soma instance segmentation and implement it

on the full brain by deploying a parallelized large-scale data processing pipeline. We hope this benchmark work could benefit the future study of the drosophila neural system.

Acknowledgement

We thank Prof. Feng Wu, Prof. Xiaoyan Sun, and Prof. Xuejin Chen for advice in the method design, Dr. Haitao Chu, Dr. Xinwei Zheng, Dr. Haifeng Liu, Feng Chang, and Pingbo Yuan for support in the computing platform, and all Ph.D. and Master students in our working group for the dataset annotation.

References

- [1] Birgitte Bo Andersen, Hans Jørgen G Gundersen, and Bente Pakkenberg. Aging of the human cerebellum: a stereological study. *Journal of Comparative Neurology*, 2003. [1](#)
- [2] J Douglas Armstrong and Jano I van Hemert. Towards a virtual fly brain. *Philosophical Transactions of the Royal Society A: Mathematical, Physical and Engineering Sciences*, 2009. [1](#)
- [3] J Alexander Bae, Mahaly Baptiste, Agnes L Bodor, Derrick Brittain, JoAnn Buchanan, Daniel J Bumbarger, Manuel A Castro, Brendan Celii, Erick Cobos, Forrest Collman, et al. Functional connectomics spanning multiple areas of mouse visual cortex. *bioRxiv*, 2021. [1](#)
- [4] Daniel R Berger, H Sebastian Seung, and Jeff W Lichtman. Vast (volume annotation and segmentation tool): efficient manual and semi-automatic labeling of large 3d image stacks. *Frontiers in neural circuits*, 2018. [3](#)
- [5] Rolf Bodmer and Yuh Nung Jan. Morphological differentiation of the embryonic peripheral neurons in drosophila. *Roux's archives of developmental biology*, 1987. [1](#)
- [6] Thomas Burne, E Scott, Bruno van Swinderen, M Hilliard, Judith Reinhard, Charles Claudianos, D Eyles, and John McGrath. Big ideas for small brains: what can psychiatry learn from worms, flies, bees and fish? *Molecular psychiatry*, 2011. [1](#)
- [7] Sebastian Busch, Mareike Selcho, Kei Ito, and Hiromu Tanimoto. A map of octopaminergic neurons in the drosophila brain. *Journal of Comparative Neurology*, 2009. [1](#)
- [8] Sebastian Cachero, Aaron D Ostrovsky, Y Yu Jai, Barry J Dickson, and Gregory SXE Jefferis. Sexual dimorphism in the fly brain. *Current biology*, 2010. [1](#)
- [9] Ann-Shyn Chiang, Chih-Yung Lin, Chao-Chun Chuang, Hsiu-Ming Chang, Chang-Huain Hsieh, Chang-Wei Yeh, Chi-Tin Shih, Jian-Jheng Wu, Guo-Tzau Wang, Yung-Chang Chen, et al. Three-dimensional reconstruction of brain-wide wiring networks in drosophila at single-cell resolution. *Current biology*, 2011. [3](#)
- [10] Michael H Dickinson and Florian T Muijres. The aerodynamics and control of free flight manoeuvres in drosophila. *Philosophical Transactions of the Royal Society B: Biological Sciences*, 2016. [1](#)
- [11] Sven Dorkenwald, Claire E McKellar, Thomas Macrina, Nico Kemnitz, Kisuk Lee, Ran Lu, Jingpeng Wu, Sergiy Popovych, Eric Mitchell, Barak Nehoran, et al. Flywire: online community for whole-brain connectomics. *Nature Methods*, 2022. [2](#)
- [12] Jan Funke, Fabian Tschopp, William Grisaitis, Arlo Sheridan, Chandan Singh, Stephan Saalfeld, and Srinivas C Turaga. Large scale image segmentation with structured loss based deep learning for connectome reconstruction. *IEEE transactions on pattern analysis and machine intelligence*, 2018. [1](#), [2](#)
- [13] Miguel Á García-Cabezas, Yohan J John, Helen Barbas, and Basilis Zikopoulos. Distinction of neurons, glia and endothelial cells in the cerebral cortex: an algorithm based on cytological features. *Frontiers in neuroanatomy*, 2016. [1](#)
- [14] George L Gerstein. Analysis of firing patterns in single neurons. *Science*, 1960. [1](#)
- [15] R Keating Godfrey, Mira Swartzlander, and Wulfila Gronenberg. Allometric analysis of brain cell number in hymenoptera suggests ant brains diverge from general trends. *Proceedings of the Royal Society B*, 2021. [1](#), [7](#)
- [16] Eyal Gruntman and Glenn C Turner. Integration of the olfactory code across dendritic claws of single mushroom body neurons. *Nature neuroscience*, 2013. [1](#)
- [17] Volker Hartenstein. Morphological diversity and development of glia in drosophila. *Glia*, 2011. [1](#)
- [18] Suzanaerculano-Houzel and Roberto Lent. Isotropic fractionator: a simple, rapid method for the quantification of total cell and neuron numbers in the brain. *Journal of Neuroscience*, 2005. [1](#)
- [19] Wei Huang, Chang Chen, Zhiwei Xiong, Yueyi Zhang, Xuejin Chen, Xiaoyan Sun, and Feng Wu. Semi-supervised neuron segmentation via reinforced consistency learning. *IEEE Transactions on Medical Imaging*, 2022. [2](#)
- [20] Wei Huang, Shiyu Deng, Chang Chen, Xueyang Fu, and Zhiwei Xiong. Learning to model pixel-embedded affinity for homogeneous instance segmentation. In *AAAI*, 2022. [2](#)
- [21] Kei Ito, Kazunori Shinomiya, Masayoshi Ito, J Douglas Armstrong, George Boyan, Volker Hartenstein, Steffen Harzsch, Martin Heisenberg, Uwe Homberg, Arnim Jenett, et al. A systematic nomenclature for the insect brain. *Neuron*, 2014. [3](#), [7](#)
- [22] Masayoshi Ito, Naoki Masuda, Kazunori Shinomiya, Keita Endo, and Kei Ito. Systematic analysis of neural projections reveals clonal composition of the drosophila brain. *Current Biology*, 2013. [1](#), [7](#)
- [23] Michał Januszewski, Jörgen Kornfeld, Peter H Li, Art Pope, Tim Blakely, Larry Lindsey, Jeremy Maitin-Shepard, Mike Tyka, Winfried Denk, and Viren Jain. High-precision automated reconstruction of neurons with flood-filling networks. *Nature methods*, 2018. [1](#), [2](#)
- [24] Kisuk Lee, Jonathan Zung, Peter Li, Viren Jain, and H Sebastian Seung. Superhuman accuracy on the snemi3d connectomics challenge. *arXiv*, 2017. [2](#)
- [25] Roberto Lent, Frederico AC Azevedo, Carlos H Andrade-Moraes, and Ana VO Pinto. How many neurons do you have? some dogmas of quantitative neuroscience under revision. *European Journal of Neuroscience*, 2012. [1](#)
- [26] Peter H Li, Larry F Lindsey, Michał Januszewski, Mike Tyka, Jeremy Maitin-Shepard, Tim Blakely, and Viren Jain. Automated reconstruction of a serial-section em drosophila brain with flood-filling networks and local realignment. *Microscopy and Microanalysis*, 2019. [2](#)
- [27] Zudi Lin, Donglai Wei, Mariela D Petkova, Yuelong Wu, Zergham Ahmed, Silin Zou, Nils Wendt, Jonathan Boulanger-Weill, Xueying Wang, Nagaraju Dhanyasi, et al. Nucmm dataset: 3d neuronal nuclei instance segmentation at sub-cubic millimeter scale. In *MICCAI*. Springer, 2021. [2](#), [6](#)
- [28] Xiaoyu Liu, Bo Hu, Wei Huang, Yueyi Zhang, and Zhiwei Xiong. Efficient biomedical instance segmentation via knowledge distillation. In *MICCAI*. Springer, 2022. [2](#)

- [29] Xiaoyu Liu, Wei Huang, Yueyi Zhang, and Zhiwei Xiong. Biological instance segmentation with a superpixel-guided graph. In *IJCAI*, 2022. 2
- [30] Sergio Luengo-Sanchez, Concha Bielza, Ruth Benavides-Piccione, Isabel Fernaud-Espinosa, Javier DeFelipe, and Pedro Larrañaga. A univocal definition of the neuronal soma morphology using gaussian mixture models. *Frontiers in Neuroanatomy*, 2015. 1
- [31] Alessandro Motta, Manuel Berning, Kevin M Boergens, Benedikt Staffler, Marcel Beining, Sahil Loomba, Philipp Hennig, Heiko Wissler, and Moritz Helmstaedter. Dense connectomic reconstruction in layer 4 of the somatosensory cortex. *Science*, 2019. 1
- [32] Shang Mu, Szi-chieh Yu, Nicholas L Turner, Claire E McKellar, Sven Dorkenwald, Forrest Collman, Selden Koolman, Merlin Moore, Sarah Morejohn, Ben Silverman, et al. 3d reconstruction of cell nuclei in a full drosophila brain. *bioRxiv*, 2021. 1, 2, 6, 7
- [33] Suphakit Niwattanakul, Jatsada Singthongchai, Ekkachai Naenudorn, and Supachanun Wanapu. Using of jaccard coefficient for keywords similarity. In *Proceedings of the international multiconference of engineers and computer scientists*, 2013. 6
- [34] Tyler A Ofstad, Charles S Zuker, and Michael B Reiser. Visual place learning in drosophila melanogaster. *Nature*, 2011. 1
- [35] Tomoko Ohyama, Casey M Schneider-Mizell, Richard D Fetter, Javier Valdes Aleman, Romain Franconville, Marta Rivera-Alba, Brett D Mensh, Kristin M Branson, Julie H Simpson, James W Truman, et al. A multilevel multimodal circuit enhances action selection in drosophila. *Nature*, 2015. 1
- [36] David Oswald and Scott Waddell. Olfactory learning skews mushroom body output pathways to steer behavioral choice in drosophila. *Current opinion in neurobiology*, 2015. 1
- [37] Hania J Pavlou and Stephen F Goodwin. Courtship behavior in drosophila melanogaster: towards a ‘courtship connectome’. *Current Opinion in Neurobiology*, 2013. 1
- [38] Karlheinz Rein, Malte Zöckler, Michael T Mader, Cornelia Grübel, and Martin Heisenberg. The drosophila standard brain. *Current Biology*, 2002. 1
- [39] Alexander Shapson-Coe, Michał Januszewski, Daniel R Berger, Art Pope, Yuelong Wu, Tim Blakely, Richard L Schalek, Peter H Li, Shuohong Wang, Jeremy Maitin-Shepard, et al. A connectomic study of a petascale fragment of human cerebral cortex. *BioRxiv*, 2021. 1
- [40] Julie H Simpson. Mapping and manipulating neural circuits in the fly brain. *Advances in genetics*, 2009. 1
- [41] Shin-ya Takemura, Yoshinori Aso, Toshihide Hige, Allan Wong, Zhiyuan Lu, C Shan Xu, Patricia K Rivlin, Harald Hess, Ting Zhao, Toufiq Parag, et al. A connectome of a learning and memory center in the adult drosophila brain. *Elife*, 2017. 1
- [42] Shin-ya Takemura, C Shan Xu, Zhiyuan Lu, Patricia K Rivlin, Toufiq Parag, Donald J Olbris, Stephen Plaza, Ting Zhao, William T Katz, Lowell Umayam, et al. Synaptic circuits and their variations within different columns in the visual system of drosophila. *Proceedings of the National Academy of Sciences*, 2015. 1
- [43] Yucheng Tang, Dong Yang, Wenqi Li, Holger R Roth, Bennett Landman, Daguang Xu, Vishwesh Nath, and Ali Hatamizadeh. Self-supervised pre-training of swin transformers for 3d medical image analysis. In *CVPR*, 2022. 6
- [44] Wynand van der Goes van Naters and John R Carlson. Receptors and neurons for fly odors in drosophila. *Current biology*, 2007. 1
- [45] Donglai Wei, Zudi Lin, Daniel Franco-Barranco, Nils Wendt, Xingyu Liu, Wenjie Yin, Xin Huang, Aarush Gupta, Won-Dong Jang, Xueying Wang, et al. Mitoem dataset: large-scale 3d mitochondria instance segmentation from em images. In *MICCAI*. Springer, 2020. 6
- [46] Jingpeng Wu, William M Silversmith, Kisuk Lee, and H Sebastian Seung. Chunkflow: hybrid cloud processing of large 3d images by convolutional nets. *Nature Methods*, 2021. 1, 5
- [47] Zhihao Zheng, J Scott Lauritzen, Eric Perlman, Camenzind G Robinson, Matthew Nichols, Daniel Milkie, Omar Torrens, John Price, Corey B Fisher, Nadiya Sharifi, et al. A complete electron microscopy volume of the brain of adult drosophila melanogaster. *Cell*, 2018. 1, 2